Kinematics of the tined combine harvester reel

Moses F. Oduori[1*], Thomas O. Mbuya[1], Jun Sakai[2], Eiji Inoue[2]

(1. *Department of Mechanical and Manufacturing Engineering, University of Nairobi, P. O. Box 30197, 00100 (GPO), Nairobi, Kenya*;

2. *Department of Bio-production and Environmental Science, Kyushu University, Hakozaki, Higashi-ku, Fukuoka, 812, Japan*)

Abstract: Although derivation of the kinematic equations of the combine harvester reel is readily achieved, certain inferences thereof suggest possible improvements in its kinematical design.   A mathematically computed reference value of the reel index (ratio of the product of the reel radius and rotational velocity to the reel advance velocity) is found to be larger than commonly recommended values.   The point, either spatial or temporal, within the cycle of reel motion, at which the tinebar should preferably enter the crop is discussed.   The pick-up performance of the tines is qualitatively analyzed and its possible improvement through redesign of reel tine kinematics is suggested.

Keywords: combine harvester reel, reel kinematics, tine trajectory

1   Introduction

The idea of using a revolving reel on grain reaping equipment was apparently originated by John Common of England, in the period 1811-1812 (Quick and Buchele, 1978).   Patrick Bell from Scotland, who is credited with invention of the first practical reaping machine, used a revolving slat reel on his successful machine of 1828 (Partridge, 1973).   Cyrus McCormick from the United States of America, who is credited with independent invention of a practical reaping machine, also used a revolving slat reel on his machine of 1831 (Quick and Buchele, 1978; Partridge, 1973).   In 1933, J. Edward Love and Horace D. Hume from the United States of America patented a tined pick-up reel (Quick and Buchele, 1978).   Today, the tined reel is standard equipment on most combine harvester designs.

Analyses of combine harvester reel kinematics have been presented by several authors, with Goryachkin

(1974) apparently being one of the earliest.   However, reel tine kinematics, as such, has often been discussed only graphically without presentation of the relevant equations (Kanafojski and Karwowski, 1976; Klenin, Popov and Sakun, 1985; Bosoi et al., 1991).

In this paper, a possible improvement of the pick-up performance of the tines, particularly in lodged and tangled crop, is sought through redesign of tine kinematics and tine crop interaction.   The effect of the reel index on reel tinebar trajectory, and the implication thereof on reel performance, is examined.   Moreover, within the cycle of reel motion, the timing of the entry of the reel tinebars into the crop is critically reviewed.

2   Kinematic analysis

2.1   Reference frame, assumptions and definitions

Figure 1 shows a profile of the tined combine harvester reel showing the coordinate reference frame and the parameters that are relevant to the kinematic analysis.   The following assumptions are made in the kinematic analysis,

1) The reel rotates about its lateral axis at a constant angular velocity, ω (rad/s), taken to be positive in the clockwise sense.

2) The reel advances into the crop in the positive X direction, over plane horizontal ground and at uniform velocity, V.

3) The tine has no rotational motion relative to the fixed Cartesian coordinate reference frame.
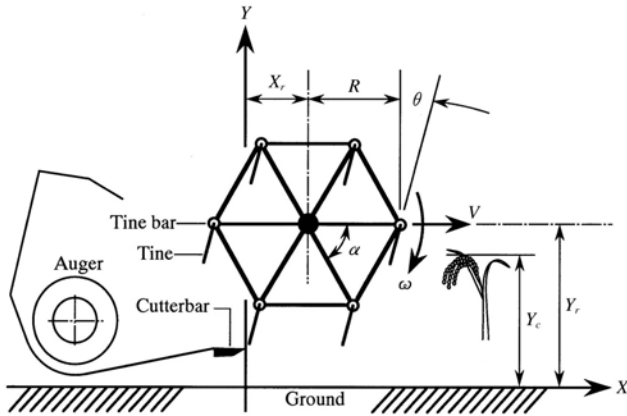
Figure 1   The conventional tined combine harvester reel with the coordinate reference frame and the parameters relevant to the analysis of its motion

It follows that the motion of the reel is two-dimensional. Furthermore, on current tined combine harvester reels, the tines are usually constrained to translate without rotating, with the tine rake angle, θ, being pre-selected.

2.2   Plane displacement as a linear transformation

In Figure 2, the movable plane Cartesian coordinate reference frame, $X'Y'$, whose origin is initially at O', is embedded in a rigid body that is undergoing a general finite plane displacement, consisting of a translation and a rotation, relative to the fixed plane Cartesian coordinate reference frame XY.

The point denoted P in Figure 2, is also embedded within the rigid body, and is therefore fixed relative to the movable reference frame $X'Y'$.   In general, a point in the plane Cartesian coordinates (X, Y) may be represented by the homogeneous coordinates (X^*, Y^*, k) where k is any positive real number (Paul, 1981; Pettofrezzo, 1978) such that:

$$X = X^*/k \quad \text{and} \quad Y = Y^*/k$$

The situation is much simplified if k is taken to be unity.   Given this notation, the displacement of point P in Figure 2 may be represented by the following linear transformation:

$$\begin{Bmatrix} X_2 \\ Y_2 \\ 1 \end{Bmatrix} = \begin{bmatrix} \cos\beta & \sin\beta & (X_0 + \Delta X_0) \\ -\sin\beta & \cos\beta & (Y_0 + \Delta Y_0) \\ 0 & 0 & 1 \end{bmatrix} \begin{Bmatrix} X_1 - X_0 \\ Y_1 - Y_0 \\ 1 \end{Bmatrix}$$

(1)

in which the three by three square matrix may be regarded as a plane displacement matrix.   This approach is found to be convenient in the analysis of tined reel kinematics.
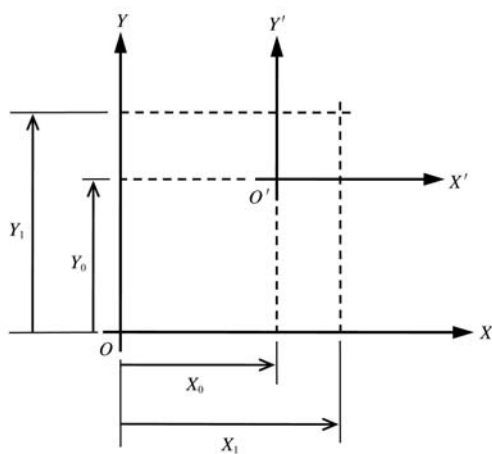
a. Initial position of point P b. Position of point P after a general plane displacement
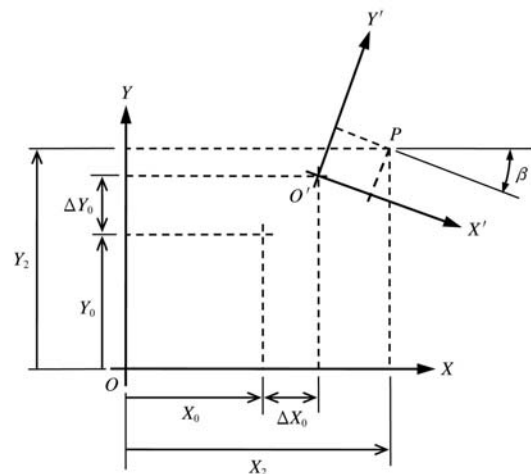
Figure 2   Representation of displacement in the plane

2.3   Tine and tinebar kinematics

In Figure 3, the position of a tine is specified by the positions of its hinge (actually the axis of its hinge), denoted by H and its tip denoted by T.   The tine hinge is also taken to represent the position of the tinebar. Starting with the tine hinge at $H(0)$ when $t = 0$, the

trajectories of the hinge and tip are shown in the figure for one complete cycle.
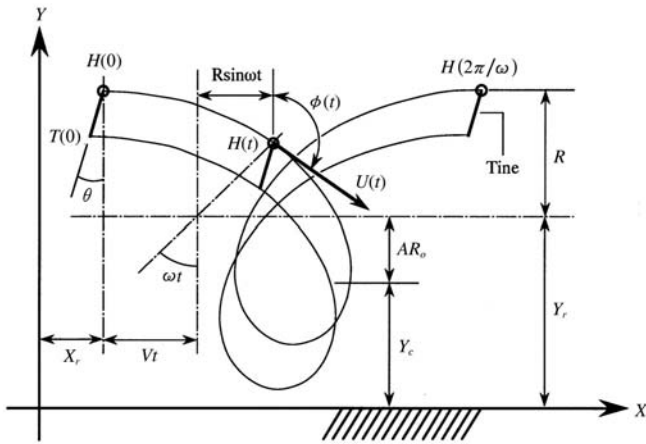
Figure 3   Trajectories of a tine hinge and tip.
H denotes hinge, T denotes tip and t denotes time.

Appropriate application of Equation (1) to Figure 3 yields the following trajectory equation:

$$\begin{Bmatrix} X \\ Y \\ 1 \end{Bmatrix}_H = \begin{bmatrix} \cos\omega t & \sin\omega t & (X_r + Vt) \\ -\sin\omega t & \cos\omega t & Y_r \\ 0 & 0 & 1 \end{bmatrix} \begin{Bmatrix} 0 \\ R \\ 1 \end{Bmatrix} \quad (2)$$

where the subscript H denotes hinge.   Denoting the length of the tine by L, the corresponding trajectory of the tip is found by imposing an appropriate translation from the trajectory of the hinge as obtained above, and is as follows:

$$\begin{Bmatrix} X \\ Y \\ 1 \end{Bmatrix}_T = \begin{bmatrix} \cos\omega t & \sin\omega t & (X_r - L\sin\theta + Vt) \\ -\sin\omega t & \cos\omega t & (Y_r - L\cos\theta) \\ 0 & 0 & 1 \end{bmatrix} \begin{Bmatrix} 0 \\ R \\ 1 \end{Bmatrix}$$

$$(3)$$

Here, let us introduce the following notation:

$$R_0 = V/\omega$$

In the above expression, the quantity R_0 is a displacement whose magnitude is equal to the header advance per radian of reel rotation.   Although the unit of R_0 can be stated as metres per radian, R_0 has the dimensions of a length since the radian is a dimensionless quantity.   Therefore, in mathematical expressions, R and R_0 can be treated as quantities of the same kind without violating the requirement of dimensional homogeneity.

It can be shown, by graphical plots, for instance, that the trajectories defined by Equation (2) and Equation (3) are looped trochoids provided that $0<R_0<R$.   When $R_0=R$,

the loops in the trochoidal trajectories will be reduced to points and the reel will not perform the function of gathering the crop properly.   Moreover, when $R_0=0$, the implication is that the reel rotates without advancing into the crop and, again, it will not perform the crop-gathering function properly (see Section 3.1 in this paper).

Corresponding velocity and acceleration equations are found, respectively, by successively differentiating the displacement matrix with respect to time.   It is to be expected that the velocities and accelerations of the hinge and the tip of a given tine turn out to be equal, since the tine translates without rotating.   The appropriate equations are as follows:

$$\begin{Bmatrix} U_x \\ U_y \\ 0 \end{Bmatrix} = \begin{bmatrix} -\omega\sin\omega t & \omega\cos\omega t & V \\ -\omega\cos\omega t & -\omega\sin\omega t & 0 \\ 0 & 0 & 0 \end{bmatrix} \begin{Bmatrix} 0 \\ R \\ 1 \end{Bmatrix} \quad (4)$$

where the three by three square matrix may be thought of as a velocity matrix, and:

$$\begin{Bmatrix} a_x \\ a_y \\ 0 \end{Bmatrix} = \begin{bmatrix} -\omega^2\cos\omega t & -\omega^2\sin\omega t & 0 \\ \omega^2\sin\omega t & -\omega^2\cos\omega t & 0 \\ 0 & 0 & 0 \end{bmatrix} \begin{Bmatrix} 0 \\ R \\ 1 \end{Bmatrix} \quad (5)$$

where the three by three square matrix may be thought of as an acceleration matrix.   Thus, expressions for the X and Y components and hence the magnitudes and directions of both velocity and acceleration may be readily derived.

3   Discussion

3.1   Reel index

The reel index, usually denoted by K and equal to $\omega R/V$ or R/R_0, is an often used parameter in analyses of reel motion and performance.   The suitable value of this index should vary with the crop and crop conditions but values lower than 1.5 are often recommended.   The effect of the value of the reel index on the geometrical form of the reel tinebar trajectory and its implications on reel performance should be taken into the consideration.

It was stated in section 2.3 that the limits of R_0 are $0<R_0<R.$.   This sets the theoretical limits of the reel index to be $1<K<\infty$.

In Figure 4, the X components of tinebar velocity become zero at both points $H(t_1)$ and $H(t_3)$.
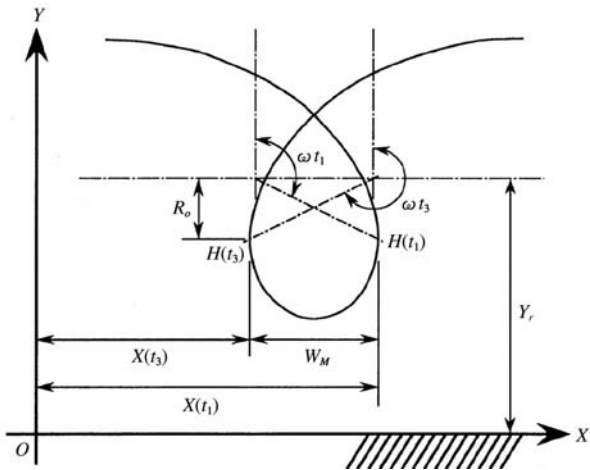
Figure 4   Maximum width across the trochoid loop

Furthermore, it should be evident in Figure 4 that $\omega t_1 + \omega t_3 = 2\pi$ radians.   These facts can be used together with the equations of tinebar trajectory to obtain the following equation:

$$\frac{W_M}{2R} = \sqrt{1 - \left(R_0/R\right)^2} - \frac{R_0}{R}\cos^{-1}\left(R_0/R\right) \qquad (6)$$

and through curve-fitting (Figure 5), Equation (6) may be simplified to:

$$\frac{W_M}{2R} = \left[1 - \left(R_0/R\right)\right]^{1.55} \qquad (7)$$

In both Equations (6) and (7), it is evident that for $R_0 = R$, $W_M = 0$ and the loop in the trochoidal trajectory disappears.   Moreover, for $R_0 = 0$, $W_M = 2R$, which implies that the reel rotates without advancing into the crop.   This is in agreement with the limits $0 < R_0 < R$ that were earlier encountered in Section 2.3 of this paper.
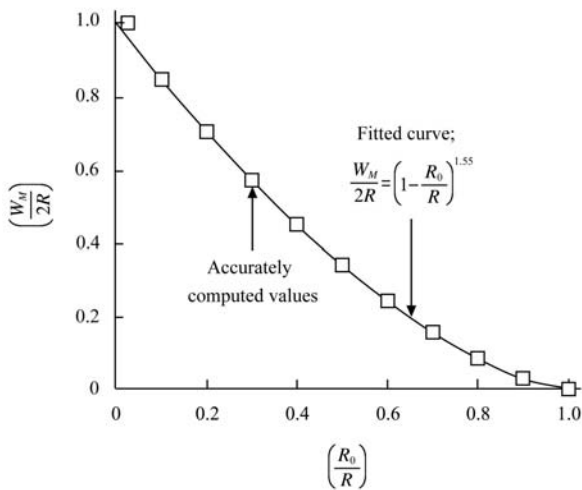
Figure 5   Curve fitted to the expression for the width of the loop
in the trochoidal trajectory

According to the mean value theorem of the integral calculus (Zill, 1985), the mean value $\mu(y)$ of a function $y=f(x)$ that is continuous on the open interval (x_1, x_2) is given by:

$$\mu(y) = \frac{1}{x_2 - x_1}\int_{x_1}^{x_2} f(x)\mathrm{d}x \qquad (8)$$

Therefore, within the practical limits of the ratio R_0/R, that is $0 < R_0/R < 1$, the mean value of the left-hand side of Equation (7), which is akin to the mean value of the width across the trochoid loop, may be computed as follows:

$$\mu\left(\frac{W_M}{2R}\right) = \int_0^1 \left[1 - \left(R_0/R\right)\right]^{1.55}\mathrm{d}(R_0/R) = 0.392 \qquad (9)$$

By substituting this value for the left-hand side of Equation (7), one finds that:

$$\mu\left(\frac{R_0}{R}\right) = 0.453 \qquad (10)$$

Now since the ratio R_0/R is the reciprocal of the real index, it follows that:

$$\mu(K) = \frac{1}{\mu(R_0 / R)} = 2.2 \qquad (11)$$

and that the value of the reel index, as computed above, which corresponds to the mean value of the width across the trochoid loop, is considerably higher than some of the values that are often recommended.

Using values of the reel index that are lower than the value computed above implies using a correspondingly smaller width of the trochoidal loop, which in turn implies that the reel gathers a correspondingly smaller quantity of crop per cycle of its motion.   There appears to be motivation for using larger values of the reel index, in order to maximize the time rate of the crop reaping operation.   However, this argument is based entirely on reel motion and does not consider aspects of reel performance such as crop losses, which the authors have discussed elsewhere (Oduori et al., 2008; Oduori, 1994).   While a higher reel index may be favourable from the point of view of maximizing the time rate of the crop reaping operation, it may be found to be unfavourable from the point of view of minimizing crop losses.   Like most engineering problems, the design and operation of the combine harvester reel apparently calls for some

compromises and trade-offs.

3.2   Timing of tinebar entry into the crop

By using the equations of the components of velocity, which can be obtained by expanding Equation (4), the magnitude of velocity of hinge H at time t can be expressed as follows:

$$U = \sqrt{1 + 2(R/R_0)\cos \omega t + (R/R_0)^2} \qquad (12)$$

and the direction of this velocity may be expressed as follows:

$$\varphi = \tan^{-1}\left[\frac{(R_0/R) + \cos \omega t}{\sin \omega t}\right] \qquad (13)$$

The quantities expressed by Equations (12) and (13) are also illustrated in Figure 6.
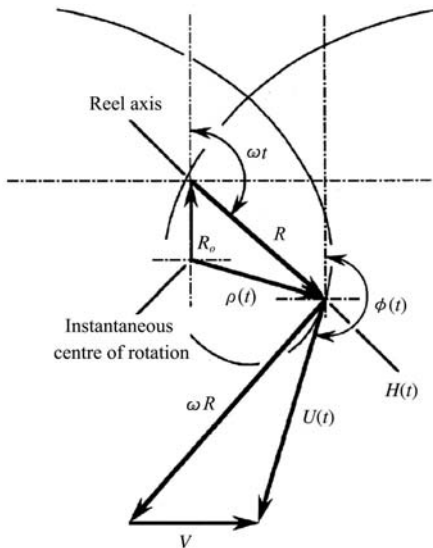
Figure 6   Vector diagram of tinebar position and velocity

In Figure 6, the following vector equations hold:

$$\omega \times R_0 = V \quad \text{and} \quad \omega \times \rho(t) = U(t) \qquad (14)$$

and therefore $\rho(t)$ and $U(t)$ are always perpendicular to each other.

Goryachkin (1974) postulated that a reel slat (or tinebar) should preferably be made to enter the crop at the moment in time, denoted t_1, when its velocity vector is directed in the negative Y direction.   This postulate leads to the following equation:

$$Y_r = Y_c + R_0 \qquad (15)$$

and:

$$U(t_1) = V\sqrt{(R/R_0)^2 - 1} \qquad (16)$$

Equation (15) is illustrated in Figure 7a.
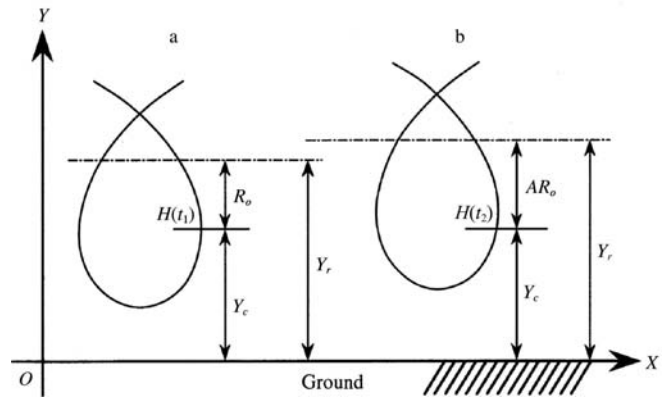
Figure 7   Height of the reel's axis above the ground

More generally, the constraint that a tinebar should be made to enter the crop with its velocity vector directed in the negative Y direction may be done away with.   The tinebar is then considered to enter the crop at a moment in time, denoted t_2, such that its velocity vector has a negative Y component and the following relations hold:

$$Y_r = Y_c + AR_0 \qquad (17)$$

$$U(t_2) = V\sqrt{1 - 2A + (R/R_0)^2} \qquad (18)$$

and:

$$\varphi(t_2) = \tan^{-1}\left[\frac{A - 1}{\sqrt{(R/R_0)^2 - A^2}}\right] \qquad (19)$$

Equation (17) is illustrated in Figure 7b.   The quantity denoted A is a dimensionless number whose value is defined by Equation (17), and can be controlled in field experiments by adjusting the height of the reel axis above ground level.   Equations (15) and (16) are then seen to be special cases of Equations (17) and (18), respectively, when A is set to unity.

Goryachkin's postulate is based on the direction of velocity of the tinebar at the moment of entry into the crop but does not consider the magnitude of that same velocity.   However, the percentage of grains shattered from grain ears by impact, has been observed to increase approximately in direct proportion to the square of the magnitude of impact velocity.   Therefore, minimization of crop losses should involve the manipulation of both the magnitude and the direction of tinebar velocity (Oduori et al., 2008; Oduori, 1994).

At the instant of tinebar entry into the crop, Figure 8 illustrates the variation in the magnitude of tinebar

velocity with A, for different values of the reel index, K. It can be seen in the figure that values of $U(t_2)$ increasingly fall below the value of $U(t_1)$ as the value of A is increased above unity.   However, as A is increased above unity, the values of $U(t_2)$ decrease at slower rates for higher values of the real index.   Therefore the value of $U(t_2)$ can be decreased either by increasing A, or decreasing K, or both.
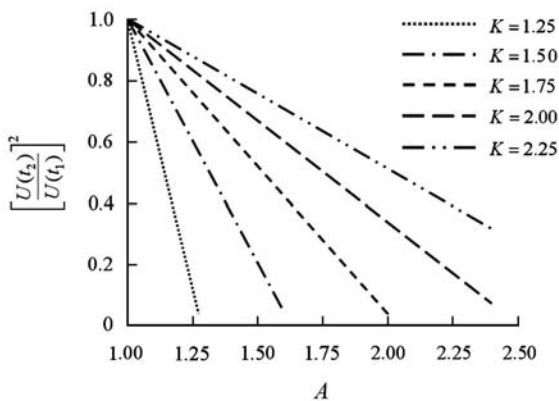
Figure 8   Variation of the magnitude of velocity of tinebar entry into the crop with A, for various values of the reel index, K

Figure 9 similarly illustrates the variation in the direction of tinebar velocity, as indicated by $\phi(t_2)$, with A. It can be seen in the figure that the value of $\phi(t_2)$, measured in degrees, increases as A is increased, and reaches a value of 270 degrees, as A becomes equal to K, but does so at a slower rate for higher values of K.   A value of $\phi(t_2)=270°$ implies that the reel tinebar does not enter the crop at all.   Therefore, in practice the value of A has to be substantially lower than K.
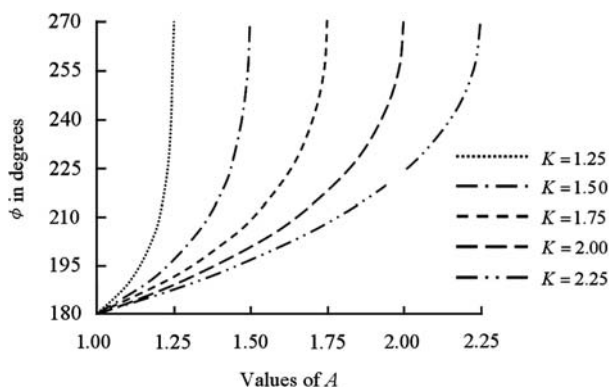
Figure 9   Variation of the direction of velocity of tinebar entry into the crop with A, for various values of the reel index, K

The suitable value of A to be preferred cannot be

discerned from a purely kinematic analysis and should involve an empirical investigation of its effect on crop losses (Oduori et al., 2008; Oduori, 1994).

3.3   Tine rake angle and tine pick-up performance

The tined pick-up reel, as compared to the slat reel, should be of greatest advantage when used in lodged and tangled crop.   The pick-up function of the tines may be analyzed in three essential stages as follows.

1) *Penetration* of the tines into lodged and tangled crop foliage.   This is necessary if the tines are to subsequently feed the crop to the cutterbar and then convey the cut crop to the gathering table.   Penetration should occur as the tines descend into the crop.   Tine motion should be directed along the tine axes for most effective penetration.

2) *Feeding* the crop to the cutterbar and gathering table by a lifting and raking action.   During this stage the tines should be adequately angled from the vertical direction so as to be able to support and lift the crop against the force of gravity.

3) *Release* of the already cut crop onto the gathering table.   This should be timely in order to avoid the possibility of the crop being carried around and over the reel, only to be deposited on the ground ahead of the header.   During this stage the tines should preferably be directed vertically downwards.

Each of the above three stages calls for a tine orientation that is contradictory with the requirements of the other two stages.   The current practice of utilizing a preset tine rake angle that does not vary throughout the cycle of reel motion may not the most appropriate.   A re-design of tine kinematics may possibly lead to better reel performance.   Figure 10 illustrates a design of tine kinematics that attempts to fulfill the requirements implied by the above analysis.   However, whether this will work better than the existing designs or not can only be ascertained through experimentation.

The following equations were used in the derivation of Figure 10.

$$X_T(t) = X_r + Vt + R\sin\omega t - L\sin\theta(t) \qquad (20)$$

$$Y_T(t) = Y_r + R\cos\omega t - L\cos\theta(t) \qquad (21)$$

In Equ. (20) and (21), for $[\pi - \cos^{-1}(R_0/R)] \leq \omega t \leq \pi$:

$$\tan\theta(t) = -\left[\frac{(R_0 / R) + \cos\omega t}{\sin\omega t}\right] \qquad (22)$$

and for $\pi \le \omega t \le [\pi + \cos^{-1}(R_0 / R)]$:

$$\tan\theta(t) = \left[\frac{(R_0 / R) + \cos(2\pi - \omega t)}{\sin(2\pi - \omega t)}\right] \qquad (23)$$

while for all other values of ωt, $\theta(t)$ was set to zero. Furthermore, the X_H and Y_H were as given by Equation (2).

Equation (22) ensures that tine motion is directed along the tine axis during its descent into the crop in order to facilitate penetration. On the other hand, Equation (23) progressively reduces the angle made by the tine with the vertical, as the tine ascends from its lowest position, until the tine becomes vertical again.

a. Conventional tine kinematics

b. Proposed improved tine kinematics
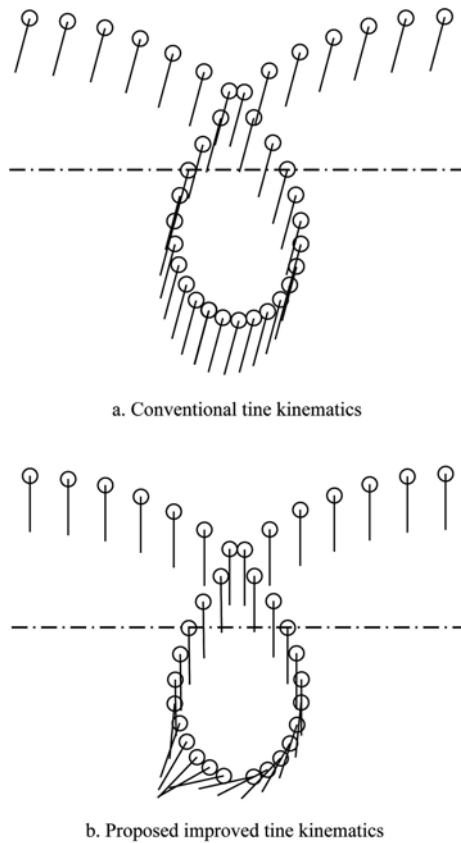
Figure 10   A possible re-design of reel tine kinematics

4   Conclusions

1) The equations obtained in this study should prove to be useful in further studies on aspects of reel design and operation. Based on these equations, a redesign of combine harvester reel tine kinematics in an attempt to improve the tines' pick-up performance is proposed. A mathematical solution for such a redesign has been presented, though a mechanical design is yet to be done. Whether the proposed design will actually improve combine harvester reel performance or not can only be determined through experimentation.

2) By considering reel kinematics alone, a value of the reel index that leads to a mean value of the width across the trochoidal loop in the tinebar trajectory was computed. Using the value of the reel index so computed as a reference value, higher values of the reel index would increase the width across the trochoidal loop, and possibly increase the amount of crop that is gathered by the real in a single cycle of its motion, and vice versa. There may be some scope for the use of higher values of the reel index. However, the reel index should not be increased without due regard to its effect on crop losses.

3) Based on the equations of reel kinematics, the postulate that the tinebar should be made to enter the crop with a velocity that is directed vertically downwards was reviewed. This postulate needs to be critically investigated in the context of its implications on crop losses.

Notation

a_x, a_y components of tinebar acceleration (m s^{-2})

A factor relating height of the crop to height of the axis of the reel above the ground (dimensionless)

f generic notation for mathematical functions

K the reel index (dimensionless)

L length of a tine (m)

R radius of reel (m)

R_0 a distance whose magnitude is equal to the header advance per radian of reel rotation (m)

t time (s)

$U(t)$ magnitude of tinebar velocity (m s^{-1})

U_x, U_y components of tinebar velocity (m s^{-1})

V header advance velocity (m s^{-1})

W_M maximum width across the loop in the trochoidal trajectory (m)

X, Y Cartesian coordinates in the plane (m)

X_r, Y_r Cartesian coordinates of the initial position of the axis of rotation of the reel in the plane relative to the coordinate reference frame (m)

$X(t)$, $Y(t)$ components of the position vector of a point moving in the plane (m)

Y_c effective height of the crop (m)

β rotational displacement in the plane (rad)

ΔX, ΔY components of translational displacement in the plane (m)

$\phi(t)$ direction of tinebar velocity (rad)

μ generic notation for mean value

θ tine rake angle (angle of pitch of the tines, rad)

$\rho(t)$ magnitude of the position vector of the tinebar relative to the instantaneous centre of rotation (m)

ω angular velocity of the reel (rad s^{-1})

References

Bosoi, E. S., O. V. Verniaev, I. I. Smirnov, and E. G. Sultan-Shakh. 1991. *Theory, Construction, and Calculations of Agricultural Machines*. Rotterdam, A. A. Balkema.

Goryachkin, V. P. 1974. *Collected Works in Three Volumes, vol. III*. Springfield, Virginia 22151, U.S. Department of Commerce, National Technical Information Service.

Kanafojski, Cz. and T. Karwowski. 1976. *Agricultural Machines, Theory and Construction, vol. II*. Springfield, Virginia 22151, U.S. Department of Commerce, National Technical Information Service.

Klenin, N. I., I. F. Popov, and V. A. Sakun. 1985. *Agricultural Machines*. New Delhi, Amerind Publishing Co. Pvt. Ltd.

Oduori, M. F., T. O. Mbuya, J. Sakai, and E. Inoue. 2008. Shattered rice grain loss attributable to the combine harvester reel: model formulation and fitting to field data. *Agricultural Engineering International: the CIGR EJournal*, 10.

Oduori, M. F. 1994. Basic principles of combine harvester reel design and operation. An Unpublished Ph. D. Thesis. Fukuoka, Japan: Kyushu University.

Partridge, M. 1973. *Farm Tools Through the Ages*. Osprey Publishing Ltd., Chapter 5: 126-133.

Paul, R. P. 1981. *Robot Manipulators: Mathematics, Programming and Control*. Cambridge, Massachusetts and London: The MIT Press.

Pettofrezzo, A. J. 1978. *Matrices and Transformations*. Dover Publications Incorporated, New York.

Quick, G., and W. Buchele. 1978. *The Grain Harvesters*. St. Joseph, Michigan, USA. The American Society of Agricultural Engineers, Chapter 3: 21.

Zill, D. G. 1985. *Calculus with Analytic Geometry*. Prindle, Weber and Schidt, Boston.